

A simple, compact, and rigid piezoelectric step motor with large step size

Qi Wang and Qingyou Lu

Citation: *Rev. Sci. Instrum.* **80**, 085104 (2009); doi: 10.1063/1.3197381

View online: <http://dx.doi.org/10.1063/1.3197381>

View Table of Contents: <http://rsi.aip.org/resource/1/RSINAK/v80/i8>

Published by the [American Institute of Physics](#).

Related Articles

Scanning superconducting quantum interference device on a tip for magnetic imaging of nanoscale phenomena
Rev. Sci. Instrum. **83**, 073702 (2012)

Optimal design and fabrication of three-dimensional calibration specimens for scanning probe microscopy
Rev. Sci. Instrum. **83**, 053708 (2012)

Nanotube-based scanning rotational microscope
Appl. Phys. Lett. **100**, 173101 (2012)

Methods and instrumentation for piezoelectric motors
Rev. Sci. Instrum. **83**, 033706 (2012)

Note: Circuit design for direct current and alternating current electrochemical etching of scanning probe microscopy tips
Rev. Sci. Instrum. **83**, 036105 (2012)

Additional information on *Rev. Sci. Instrum.*

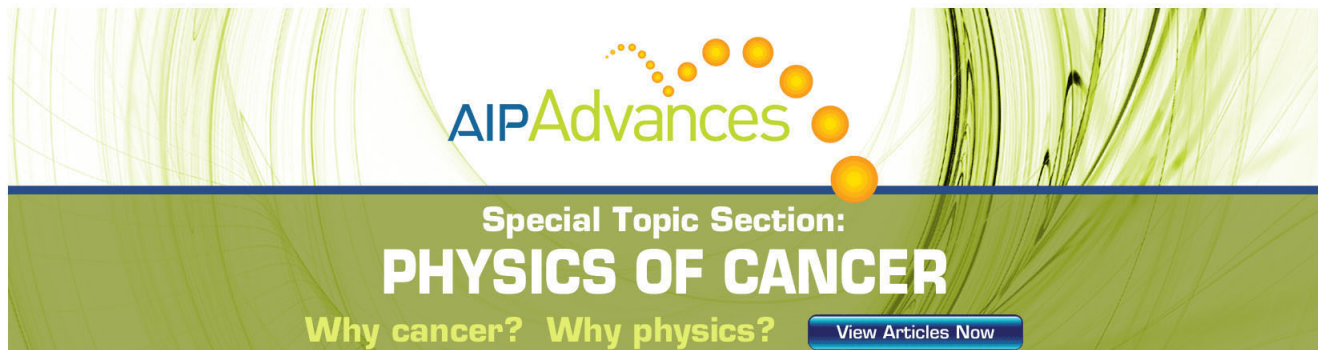
Journal Homepage: <http://rsi.aip.org>

Journal Information: http://rsi.aip.org/about/about_the_journal

Top downloads: http://rsi.aip.org/features/most_downloaded

Information for Authors: <http://rsi.aip.org/authors>

ADVERTISEMENT



AIP Advances

Special Topic Section:
PHYSICS OF CANCER

Why cancer? Why physics? [View Articles Now](#)

A simple, compact, and rigid piezoelectric step motor with large step size

Qi Wang¹ and Qingyou Lu^{1,2,a)}

¹Hefei National Laboratory for Physical Sciences at Microscale, University of Science and Technology of China, Hefei, Anhui 230026, People's Republic of China

²High Magnetic Field Laboratory, Chinese Academy of Sciences, Hefei, Anhui 230031, People's Republic of China

(Received 11 June 2009; accepted 16 July 2009; published online 14 August 2009)

We present a novel piezoelectric stepper motor featuring high compactness, rigidity, simplicity, and any direction operability. Although tested in room temperature, it is believed to work in low temperatures, owing to its loose operation conditions and large step size. The motor is implemented with a piezoelectric scanner tube that is axially cut into almost two halves and clamp holds a hollow shaft inside at both ends via the spring parts of the shaft. Two driving voltages that singly deform the two halves of the piezotube in one direction and recover simultaneously will move the shaft in the opposite direction, and vice versa. © 2009 American Institute of Physics.

[DOI: [10.1063/1.3197381](https://doi.org/10.1063/1.3197381)]

I. INTRODUCTION

The scanning probe microscope (SPM) is a powerful tool in the field of nanotechnology with some important types having atomic or even subatomic resolutions. One key component of an SPM is its coarse approach positioner which brings the tip and sample as close as in nanometer range and is many times a piezoelectric motor.^{1–11} The piezomotor has nevertheless other important applications such as mirror positioning in modern optics¹² and cell or DNA manipulations.¹³

Up to now, there are many kinds of piezomotors found in literatures including Inchworm,^{3,14–19} beetle type,^{5–7,10,20–22} shear piezostepper,^{2,8,9,11,23,24} and inertial slider,^{4,25–28} etc. However, they all have severe drawbacks. For the first three types, each needs three or more piezoelectric actuators to operate, which is too complicated in both structure and control. Their reliability and applications in small space (extreme condition environments) and weak signal measurements all become severe issues. Inertial slider is rather simple, but not very rigid (prone to vibration, thus downgrading the quality of atomic images) and unable to produce enough pushing force.

In this paper, we demonstrate a piezoelectric motor that does not have the above limitations. It is implemented by a single piezoelectric scanner tube (PST) that is axially and deeply cut into almost two halves and grips a hollow shaft (HS) inside from both ends by the spring parts of the HS. Two driving voltages that separately deform the two halves of the PST in one direction and concurrently recover will move the HS one step in the opposite direction, and vice versa. Its compactness, simplicity, rigidity, and large step size make it particularly useful in small space (extreme conditions) and low temperature applications.

II. DESIGN AND PRINCIPLE

Figure 1 shows the schematic of our design. A photo of the actual setup is given in Fig. 2. Two sapphire rings of 1.5 mm thick by 7.9 and 10.2 mm inner versus outer diameters are glued (with H74F epoxy from Epoxy Technology) onto the ends of a four-quadrant PST (model PT130.24 of Physik Instrumente, 30 mm long by 10 mm outer diameter by 0.5 mm wall thickness with ± 200 V maximum operating voltages), respectively. A cut (with diamond saw) through two opposite boundaries of the quadrants is made from the sapphire ring at one end of the PST into about 92% of the tube length toward the other end. The uncut sapphire ring is the base ring, whereas the other is cut into two semi rings which are called clamping semi rings (will clamp hold a mobile HS). Each pair of the neighboring electrodes with no cut in between is wired together, resulting in two semicylindrical electrodes, one is arbitrarily called the first electrode (E1) for convenience and the other, the second electrode (E2). The two halves of the PST that E1 and E2 control are abbreviated as P1 and P2, respectively.

The moving part of the motor is a titanium HS that is inserted into the PST as shown in Fig. 1(a). We have studied a circular and a square HS as illustrated in Fig. 1(b). For the circular one (length=45 mm, inner diameter=5.8 mm, and outer diameter=7.8 mm which can pass through the sapphire rings at the PST ends with a small gap of 0.05 mm), a wire cut through the axis is made from each end toward the other end with the cutting planes perpendicular to each other. The two cuts do not go through the entire HS and a small length of 0.8 mm remains uncut at each end. The pair of the HS cut slits having the opening toward the same direction as that of the PST slits is arranged in the same plane with the PST slits. A stronger compression spring is secured in the HS at one end, pushing the HS to open wider and press against the clamping semi rings with forces N_1 and N_2 , respectively, whereas a weaker compression spring in the HS at the other end presses the HS on the base ring with a total pressing

^{a)} Author to whom correspondence should be addressed. Tel.: 86-551-360-0247. Electronic mail: qxl@ustc.edu.cn.

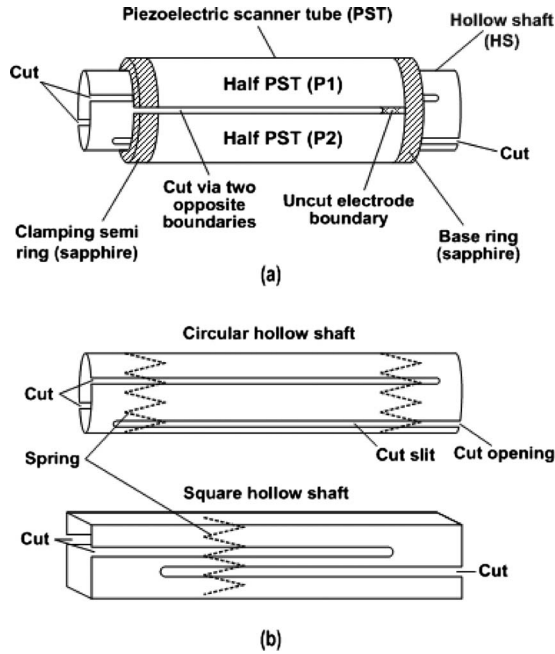


FIG. 1. (a) The structure of our piezomotor; (b) two kinds of hollow shafts studied.

force N_{br} . The three pressing forces N_1 , N_2 , and N_{br} are set roughly equal by the above stronger and weaker compression springs. Accordingly, the maximum static friction forces on the HS due to these three pressing forces are approximately equal in value (directions may be opposite as discussed below) if equal friction coefficients are assumed.

One big advantage of this mutual clamping between the PST and HS at both ends is that this structure is very firm (resistant to vibration noise) and can be installed in any direction. Also note that the clamping is elastic (long range forces), implying that large temperature variations will not change the clamping forces significantly and the three maximum static frictions remains equal in value.

To operate the motor, two driving voltages D1 and D2 of Fig. 3(a) type are applied to the electrodes E1 and E2 of the PST, respectively (the inner electrode voltage is fixed at -200 V), which will deform the corresponding semitubular actuators P1 and P2 as follows. P1 and P2 are initialized to expansion states during the first 1/6 period (T1). In T2, P2 shrinks while P1 stays unchanged. This results in a sliding between the free end of P2 and HS rather than a sliding between the base ring and HS, because the P2-to-HS maxi-

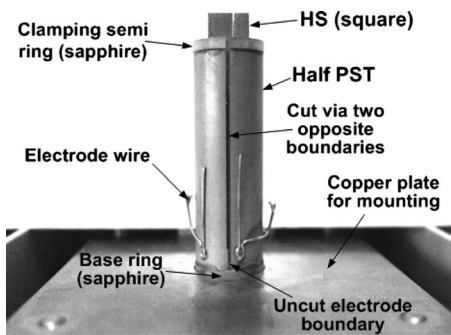


FIG. 2. The photo of our piezoelectric motor.

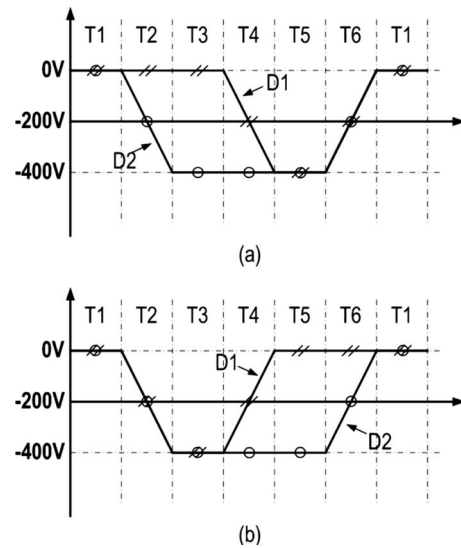


FIG. 3. (a) The two driving voltages which move the HS in the expansion direction of the PST. (b) The two driving voltages which move the HS in the contraction direction of the PST.

um static friction fr_2 is smaller than the sum of the P1-to-HS and base ring-to-HS maximum static frictions, $fr_1 + fr_{br}$ (assuming these frictions are much smaller than the blocking forces F_{b1} and F_{b2} of P1 and P2). Next, in T3, P1 and P2 both stay in the previous state. This purely “wait” state is a preparation for good synchrony in the next action, which is not necessary and can be dropped to save time. In T4, P1 shrinks while P2 stays unchanged. This induces a sliding between the free end of P1 and HS (by the similar reason to the T2 action). Up to now, both P1 and P2 have changed the states from expansion to contraction without moving the HS with reference to the base ring. T5 is another wait which is again discardable. In the last 1/6 period (T6), P1 and P2 both expand simultaneously. This time, the sliding happens only between the base ring and HS because $fr_{br} < fr_1 + fr_2$, meaning that P1 and P2 together drag the HS to move one step in the expansion direction from the base ring. Finally, P1 and P2 return to the initial states and the HS has moved one step. This sequence can be repeated to achieve a large travel range. The HS can also move in the opposite direction using the driving voltage given in Fig. 3(b) and the principle is very similar.

Apart from the circular HS described above, we have also tried a square HS (42 mm long by 5.6 mm wide, wall thickness is 0.7 mm), which is wire cut from each end to the other end (cutting length=35 mm) with the cutting planes parallel to each other, forming a serpentine structure as exhibited in Fig. 1(b). The distance between the cutting planes is 0.8 mm. This design is better than its circular counterpart in the following aspects: (1) the sliding of the HS on the sapphire rings is like ice skating shoes sliding on ice, allowing bigger pressing forces (more rigid) without increasing the frictions; (2) the frictions are better defined and more stable; (3) only one compression spring is needed, whose position in the square HS can be adjusted to meet the optimal working condition of $fr_1 \approx fr_2 \approx fr_{br}$; (4) the smallest gap

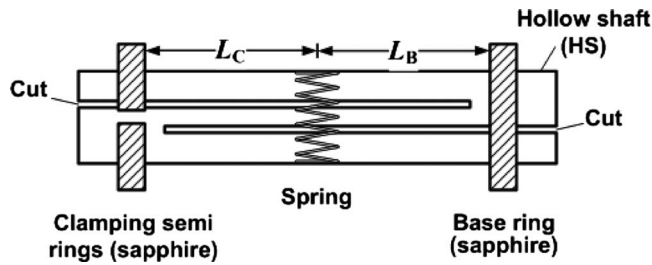


FIG. 4. The schematic diagram for deriving the range of motion.

between the square HS and the sapphire rings is easier to tweak by grinding (smaller gap will lead to a larger travel range).

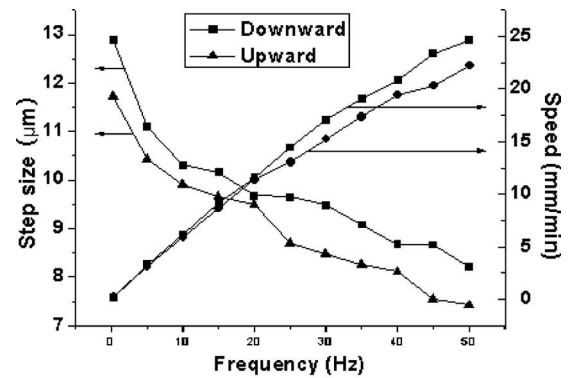
Apparently, the clamping forces N_1 , N_2 , and N_{br} do not remain constant when the HS moves, thus limiting its range of motion. The range of motion for the square HS can be derived as follows. Referring to Fig. 4 in which F_S is the force produced by the spring and L_B and L_C stand for the distances from the spring to the base ring and to the clamping semi rings, respectively, the lever law leads to: $L_B \cdot F_S = (N_1 + N_2) \cdot (L_C + L_B)$ and $L_C \cdot F_S = N_{br} \cdot (L_C + L_B)$. Because $N_1 \approx N_2$ and we need $N_1 + N_2 > N_{br}$ for the HS to walk, this means that $L_B > L_C$ should be satisfied. Since the HS cannot move if $L_C = 0$, the range of motion is finally determined by $0 < L_C < L_B$. In our design, $L_C + L_B \approx 30$ mm (the length of the PST), we expect that maximum displacement of the square HS is less than 15 mm. This issue of limitation on the range of motion can nevertheless be solved if the clamping springs are attached to the sapphire rings (not to the HS).

III. PERFORMANCE TEST

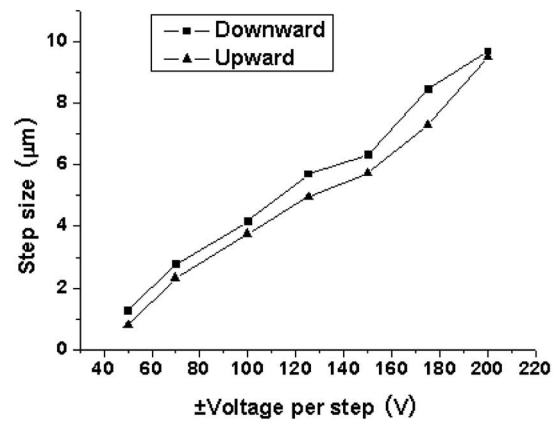
We have tested the room temperature performance of the motor in two extreme cases of moving directions (upward and downward) by measuring its step size and speed as functions of the frequency [Figs. 5(a) and 6(a) for circular and square HS, respectively] and operating voltage [Figs. 5(b) and 6(b) for circular and square HS, respectively]. The pressing forces were set to $N_1 \approx N_2 \approx N_{br} \approx 0.22$ N for circular HS which are much smaller than the blocking forces ($F_{bl1} \sim F_{bl2} \sim 2$ N) of the driving piezo-P1 and P2.

The maximum step size is $12.9 \mu\text{m}$ with the measurement conditions being: circular HS, downward stepping with 0.3 Hz driving frequency. When the moving direction is changed to upward, the step size becomes $11.7 \mu\text{m}$ due to gravity. In case of square HS, the downward and upward step sizes are 8.9 and $8.2 \mu\text{m}$, respectively, which is more uniform because of its knife edge contacts with the sapphire rings. All these step sizes are rather large compared with other types of piezoelectric motors^{9,11,23} with the similar size. The speed of motion is of course closely related to the driving frequency. The maximum driving frequency we set was 50 Hz, at which the speeds for the circular (upward versus downward) and square (upward versus downward) HS were: (22.27 versus 24.62) and (19.44 versus 19.98) mm/min.

When the driving frequency increases or if the magnitude of the operating voltage drops, the step size diminishes as seen in Figs. 5 and 6. Although we get larger step size



(a)



(b)

FIG. 5. The step size (left vertical axis) and speed (right vertical axis) of the motor using the circular HS as functions of (a) frequency (maximum operating voltage = ± 200 V) and (b) maximum operating voltage (frequency = 20 Hz).

from circular HS, we still prefer the square HS owing to its advantages listed earlier. For instance, the travel range using the square HS is 9 mm (as designed) compared with 3.3 mm for the circular HS (worse than the designed 6.6 mm travel range). The performance curves of the square HS motor seen in Fig. 6 are also smoother and more consistent than those (Fig. 5) of the circular HS motor.

Although tested in room temperature, the motor has high potential to work in liquid helium temperature for two reasons: (1) its large step size can afford to pay for the thermal contraction still with remarkable step size remaining to produce a move; (2) its spring clamping structure validates the required friction relationship, $|fr_1| \approx |fr_2| \approx |fr_{br}|$, in a very wide temperature range since a change from room temperature to liquid helium only shrinks the compression springs (~ 5 mm long, spring constant is about 286 N/m) by microns which do not considerably affect the pressing forces between the HS and the sapphire rings.

The square HS may suffer wear and tear issues as its four edges could be scratched by the sapphire rings. To test its durability, we operated the motor repeatedly with ± 200 V and 50 Hz driving voltages for more than one thousand times with a displacement about 3 mm and the motor still worked well. The wear was not severe. Of course, the HS can be coated with wear resistant materials for better protection (if necessary).

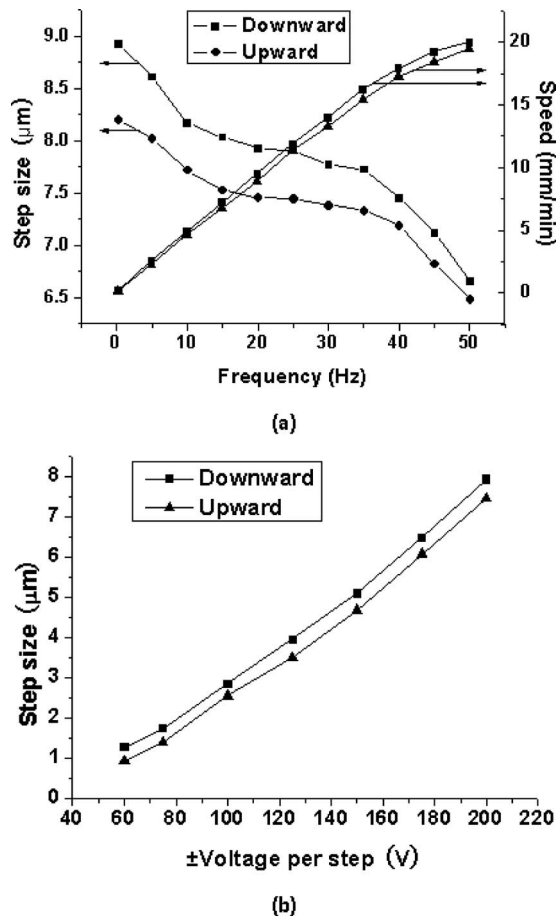


FIG. 6. The step size (left vertical axis) and speed (right vertical axis) of the motor using the square HS as functions of (a) frequency (maximum operating voltage = ± 200 V) and (b) maximum operating voltage (frequency = 20 Hz).

IV. CONCLUSION

We have presented a powerful linear piezoelectric motor that owns several important features not simultaneously owned by other piezomotors, including: large step size, small size, very rigid, simple in structure and operation, very large temperature range, easy to make and loose machining tolerance, etc. Its durability has also been tested, which is rather good. All these are highly desired in the construction of a modern SPM.

ACKNOWLEDGMENTS

This work was supported by the National Natural Science Foundation of China under Grant No. 10627403, the project of Chinese national high magnetic field facilities, and Science Foundation of The Chinese Academy of Sciences under Grant No. YZ200846.

- ¹B. J. Albers, M. Liebmann, T. C. Schwendemann, M. Z. Baykara, M. Heyde, M. Salmeron, E. I. Altman, and U. D. Schwarz, *Rev. Sci. Instrum.* **79**, 033704 (2008).
- ²Chr. Wittneven, R. Dombrowski, S. H. Pan, and R. Wiesendanger, *Rev. Sci. Instrum.* **68**, 3806 (1997).
- ³R. A. Wolkow, *Rev. Sci. Instrum.* **63**, 4049 (1992).
- ⁴Y. Hou, J. Wang, and Q. Lu, *Rev. Sci. Instrum.* **79**, 113707 (2008).
- ⁵T. H. Chang, C. H. Yang, M. J. Yang, and J. B. Dottellis, *Rev. Sci. Instrum.* **72**, 2989 (2001).
- ⁶J. H. Ferris, J. G. Kushmerick, J. A. Johnson, M. G. Yoshikawa Youngquist, R. B. Kessinger, H. F. Kingsbury, and P. S. Weisse, *Rev. Sci. Instrum.* **69**, 2691 (1998).
- ⁷N. Pertaya, K.-F. Braun, and K.-H. Rieder, *Rev. Sci. Instrum.* **75**, 2608 (2004).
- ⁸T. Hanaguri, *J. Phys.: Conf. Ser.* **51**, 514 (2006).
- ⁹S. H. Pan, E. W. Hudson, and J. C. Davis, *Rev. Sci. Instrum.* **70**, 1459 (1999).
- ¹⁰L. A. Silva, *Rev. Sci. Instrum.* **68**, 1300 (1997).
- ¹¹A. K. Gupta and K.-W. Ng, *Rev. Sci. Instrum.* **72**, 3552 (2001).
- ¹²J. Lee, J. Chae, C. K. Kim, H. Kim, S. Oh, and Y. Kuk, *Rev. Sci. Instrum.* **76**, 093701 (2005).
- ¹³J. Kusch, A. Meyer, M. P. Snyder, and Y. Barral, *Genes Dev.* **16**, 1627 (2002).
- ¹⁴Burleigh Instruments, Inc., U.S. Patent No. 3,902,084 (1975).
- ¹⁵P. E. Tenzer and R. Ben Mrad, *IEEE/ASME Trans. Mechatron.* **9**, 427 (2004).
- ¹⁶J. Frank, G. H. Koopmann, W. Chen, and G. A. Lesieutre, *Proc. SPIE* **3668**, 717 (1999).
- ¹⁷J. Ni and Z. Zhu, *IEEE/ASME Trans. Mechatron.* **5**, 441 (2000).
- ¹⁸K. Duong and E. Garcia, *Proc. SPIE* **2443**, 782 (1995).
- ¹⁹J. E. Miesner and J. P. Teter, *Proc. SPIE* **2190**, 520 (1994).
- ²⁰B. Koc, S. Cagatay, and K. Uchino, *IEEE Trans. Ultrason. Ferroelectr. Freq. Control* **49**, 495 (2002).
- ²¹M. Bexell and S. Johansson, *Sens. Actuators, A* **75**, 118 (1999).
- ²²J. Frohn, J. F. Wolf, K. Besocke, and M. Teske, *Rev. Sci. Instrum.* **60**, 1200 (1989).
- ²³M. H. Arafa, O. J. Aldraihem, and A. M. Baz, IEEE Proceedings of the Fifth International Symposium on Mechatronics and Its Applications, 2008 (unpublished), pp. 1–5.
- ²⁴S. H. Pan, International Patent Publication No. WO 93/19494 (1993).
- ²⁵R. Yoshida, Y. Okamoto, and H. Okada, *Jpn. Soc. Precision. Eng.* **68**, 536 (2002).
- ²⁶W. Zesch, R. Buchi, A. Codourey, and R. Siegwart, *Proc. SPIE* **2593**, 80 (1995).
- ²⁷D.-S. Paik, K.-H. Yoo, C.-Y. Kang, B.-H. Cho, S. Nam, and S.-J. Yoon, *J. Electroceram.* **22**, 346 (2009).
- ²⁸L. Howald, H. Rudin, and H.-J. Gijtherodt, *Rev. Sci. Instrum.* **63**, 3909 (1992).